Journal of Physics: Conference Series

PAPER • OPEN ACCESS

Experimental modal analysis of aeroelastic tailored rotor blades in different boundary conditions

To cite this article: J Gundlach and Y Govers 2019 *J. Phys.: Conf. Ser.* **1356** 012023

IOP Conf. Series: Journal of Physics: Conf. Series **1356** (2019) 012023 doi:10.1088/1742-6596/1356/1/012023

Experimental modal analysis of aeroelastic tailored rotor blades in different boundary conditions

J Gundlach[1] and Y Govers[1]

[1] German Aerospace Center (DLR), Institute of Aeroelasticity, Bunsenstraße 10, 37073 Göttingen, Germany

E-mail: janto.gundlach@dlr.de

Abstract. Bend-twist coupled blades are intended to reduce the loads on the overall wind turbine by passively adapting to current wind conditions. The coupling results from complex-design shapes and structures using advanced finite element models utilising shell and volume elements. These models are however prone to mispredict the structural dynamic behaviour of the rotor blades. In particular, normal modes with both bending and torsion contributions, as well as local vibrations of the blade shells include computational uncertainties. Therefore, in order to update flawed model parameter assumptions, a modal characterisation of blade prototypes including mode shapes is essential. In the present study results of a modal test campaign involving four identical rotor blades of 20 m length with geometric bend-twist coupling are reported. Design, realisation, and post-processing of the experiments have been carried out under careful consideration of a pre-existing FE shell model. Modal data is obtained at two different stages of the manufacturing process and for one blade in two separate boundary conditions, i.e. free-free in elastic suspensions and clamped to a test rig. Due to the high sensor density in both configurations, the identified normal modes do not only include coupled eigenforms but also mode shapes illustrating cross-sectional vibrations; the latter attributed to the deflection of the blade shells. The acquired dataset is found to be well-suited for the validation of the numerical model and represents a reliable basis for updating.

1. Introduction

The bend-twist coupling of rotor blades is considered as a promising solution for the sake of load reduction on wind turbines. Usually coupling effects are either induced by the blade geometry in terms of a swept and curved design or by exploiting the anisotropic behaviour of fibre-reinforced plastic laminates which are positioned off-axis. In general, a bend-twist coupled design leads to structurally coupled mode shapes of both bending and torsion contributions.

In order to specify aerodynamic loading induced by a given wind field properly, detailed knowledge of the deformation and thus the mode shapes of the rotor blades is essential. The common certification process of rotor blades does not however require for a modal identification of blade eigenforms. Apart from static and dynamic load tests, modal properties shall only be determined by means of the first two lowest eigenfrequencies of flapwise mode shapes and the first eigenfrequency of an edgewise mode shape [1]. As a consequence, the validation of structural FE models, regardless if built from shells or beams, is often constrained when it comes to dynamic torsional deflections; not to mention coupling effects between bending and torsion. Potential shortcomings in validation may then result in misprediction of the overall loading on wind turbines or in erroneous assessments of stability problems.

Driven by the need for validation, considerable research effort has been spent on modal testing procedures for rotor blade structures. In an extensive study with the blade mounted to a test rig, coupled mode shapes reduced to three degrees of freedom of rigid cross-sections have been identified in [2] using guided hammer excitation. Response signals are recorded by three sensors which have been roved along the length axis with the help of a support structure. The impact of boundary conditions has been explored for free-free tests [3] and for a blade section clamped in load frames [4]. Load frames are typically applied during static and dynamic load tests. For the purpose of validation, the fixation of the blade during modal testing should be well-thought, since idealised boundary conditions are difficult to meet. Being a crucial feature of experimental modal analysis, different excitation techniques have been subjected to investigations in [2] and [5]. An overview of possible sources of uncertainty during modal tests of rotor blades is provided in [6]. Present contribution follows previous work in providing modal testing methodology for validation of rotor blade models.

As part of the joint research project SmartBlades2 [7], four identical rotor blades with a demonstrative length scale of 20 metres have been manufactured by DLR. The blades passively adapt to varying wind conditions due to a geometric bend-twist coupling. Attributed to their outlined significance, the test design aims at identifying a detailed description of coupled mode shapes. Important aspects such as the appropriate choice of boundary conditions and excitation types are addressed with regard to reliable results on the one hand, and feasibility of the experiments in an quasi-industrial environment on the other hand. In the process, identification methods are applied that are efficiently used in Ground Vibration Tests (GVT) of commercial aircrafts [8, 9].

The first results of this work concerning only the first blade have been presented in [10]. In contrast to the previous report, section 2 provides insight into the whole modal test campaign. Potential advantages of the different boundary conditions are elucidated and the instrumentation layout for force input as well as for measuring the structural response is explained. Likewise, some brief comments about the applied experimental modal analysis techniques are part of this section. Section 3 contains assorted results which have been derived from the modal tests in the painted settings. The focus falls on the comparison of the four blades, which allows for assessing the repeatability of the manufacturing process, and on possible non-linear behaviour of the rotor blades in flapwise direction. Section 4 concludes the recent findings.

2. Framework of the modal test campaign

From the four blades that have been manufactured in the context of SmartBlades2 a complete set of blades serves as a rotor in open air wind turbine testing (blade #2 - blade #4), whereas operational and extreme load tests have been conducted on the first produced exemplar. The bend-twist coupling is realised by a swept and prebend shape. Some general data of the blades including their weight is provided in Table 1.

Table 1. General data of the blades.

dimensions in m			mass in kg	centre of gravity in m
length of rotor blade	19.99	blade #1[1]	1793	6.58
max. chord length	2.38	blade #2	1971	5.96
max. prebend	1.00	blade #3	1906	6.20
max. sweep	0.52	blade #4	1917	6.16

[1] values w/o finish

The modal test campaign incorporates the blades according to Table 2. Altogether six tests have been performed with the blades being suspended. These tests have been conducted at DLR in Stade, Germany, and at the National Wind Technology Center (NWTC) of the National Renewable Energy Laboratory (NREL) in Boulder, CO. In that configuration the modal properties of the blades before

and after finishing are compared. Within the process of finishing (cf. [11]) remains from the preceding manufacturing steps are removed. This includes cutting and grinding off protruding material at the leading, trailing edge, and the blade root. Afterwards, three layers of hand lay-up laminate are added in the near field of the root, the blade is coated and the cross bolts are inserted. Finally, the balancing of the blades is accomplished. Without additional masses from balancing, it is assumed that finishing raises the total mass of the blade by approximately 103 kg distributed on bolts (74 kg), coating (14 kg), and laminate (15 kg).

Table 2. Overview of modal test campaign: it is distinguished between free boundary conditions before and after the finishing process, and the first blade being attached to a test rig.

	blade #1	blade #2	blade #3	blade #4
free	x	x	x	
free w/ finish		x	x	x
test rig	x			

Blade #1 has been tested being clamped to a test rig at Fraunhofer Institute for Wind Energy Systems (IWES) in Bremerhaven, Germany. In that state mode shapes are determined in a uniquely high resolution. Furthermore, the blade is reviewed towards flapwise non-linearities.

All measurements are carried out with an LMS SCADAS III measurement system employing uniaxial IEPE acceleration sensors. In order to identify rigid body modes or the first flapwise mode of the blade mounted to a rig, accurate frequency response and phase purity at low frequencies is important. The employed accelerometers are rated down to 0.5 Hz. In preliminary work utilising a calibration shaker the phase deviation of all sensors has been quantified at low frequencies yielding less than 8° at 1 Hz, 3° at 2.5 Hz, and 1.5° at 5 Hz. The design of the different test scenarios is outlined in the following.

2.1. The free-free test scenario

Some aspects indicate a free-free test is preferential over a modal test in space-fixed constraints. First, a test in free boundary conditions is very efficient regarding time consumption. A test can be done directly after the blade has been removed from the mould. Depending on the size of the blade, sensor instrumentation is possible from the ground in the absence of aerial lifting devices while the blade is resting in cradles. No additional effort is required for attaching the blade to a hub or to load frames. If the blade is lifted only several centimetres, some excitation points are accessible from the ground as well. Owing to these factors, an entire free-free test as described here has been accomplished within a time span of less than two days for each blade. Second, the free boundary condition eases the process of model validation. Due to the compliance of test rigs, an authentic space-fixed clamping is difficult to realise. Being part of the elastic system, the dynamic properties of the test stand must be taken into account for the validation. Furthermore, in free-free tests the blade is less affected by mass loading, since the sensor cabling can be taken down from the blade in a convenient way.

As displayed in Figure 1(a), the free-free boundary condition is realised by means of an elastic suspension which is connected to lifting straps. The straps are attached to the blade within the proposed lifting areas at 0.35 m, and between 16.15 m and 16.50 m. The number of individual rubber bands in each suspension is selected with the objective of keeping all rigid body frequencies as low as possible. During the test, the blade is oriented pressure side up.

All blades are excited using an impact hammer with soft tip. In total, eight excitation points are positioned at two cross-sections at 3.7 m and 17.5 m, respectively. Edgewise hammer hits have been performed at the leading edge, as flapwise excitation is conducted at three discrete points in each section, i.e. on the girder, on the shell, and on the trailing edge. The cross-sections are selected with regard to a maximum of deflection appearing at the sensor positions predicted from the first ten mode shapes of the FE model. In order to identify rigid body modes, data is acquired using a large window size of 81.92 seconds. The processed frequency response functions are averaged from 10 hammer hits.

Additionally, in the test of blade #1 an electrodynamic shaker is applied at the same points emitting broadband random excitation. It has been found that all mode shapes are sufficiently excited for identification using the modal hammer only.

The majority of sensors are located on the pressure side of the blades. Over its total length the blade is cut in 17 sections where sensors are placed. Aside from the tip, each cut contains a single sensor pointing in edgewise direction, whereas four sensors on the pressure side are directed towards flap. The latter are distributed equally spaced along the chord at that section. In three (blade #1) to four (all other blades) sections the suction side is instrumented with two additional sensors. The applicability of the sensor distribution has been evaluated in the sense of an AutoMAC matrix of the first ten mode shapes indicating a maximum off-diagonal value of 23% [10].

(a)  (b) 

Figure 1. Blade fixation: free-free (a) and clamped to a test rig (b).

2.2. The test stand scenario

There are certain advantages of a clamped boundary condition with view to validation. First, the clamping resembles to the hub connection which applies when rotor blades are used in operation. Once derived from modal testing, modal data can be utilised in updating approaches [12]. Even if adjusted model parameters are selected reasonably, it is evident that independent updating based on modal data from differing boundary conditions brings about unequal finite element models. Having in mind the apparent resemblance of the connection, the model obtained from test rig data might be most suitable. Second, the clamping enables higher force input and other excitation techniques like snap-back and sine sweeps. On account of higher forces, the blade undergoes larger deformations such that potential non-linear behaviour may be revealed. Knowing the modal properties at larger deformations is particularly beneficial for solving the stability problem of flutter.

In Figure 1(b) the test stand is visualised. The block, which is screwed to the ground, has been designed to stand high cycle fatigue tests and static extreme load tests for blade certification. Modal testing has been conducted subsequent to static tests but before the fatigue test. The connection to the block is accomplished using the original 40 blade bolts. The metal plate is tilted by an angle of 7.5° and the pressure side is faced upwards again during testing.

In opposition of the free-free tests, electrodynamic long stroke shakers are incorporated for the purpose of excitation. To achieve a decent response of the structure, slow-paced logarithmic sine upsweeps of .5-1 oct/min in the range of 1-64 Hz are chosen as signals for single- and multi-point excitation. In the direction of flap, the sweeps are not customised to the response level of the structure as commonly done in aerospace GVTs. Thus a constant force level is induced to the blade without running into the constraints of the shaker, which is owing to the rather long travel of ±7.5 cm. The attachment points of the shakers are at 7.4 m on the girder and 11.6 m on the leading edge for flapwise

and edgewise force input, respectively. The positions have been selected with respect to exploitation of the full force capacity of the shakers on the one hand, and their maximum peak-to-peak travel on the other hand. Shaker positioning is realised with the help of heavyweight support platforms (see Figure 2). A less powerful shaker with ±2.5 cm travel is applied edgewise at the height of 6 metres. Large orthogonal displacements occur at the driving point when the sweep signal passes eigenfrequencies of flapwise bending modes. This is the reason for customising the excitation signal so as to ramp down the force amplitude at these frequencies (cf. [13]).

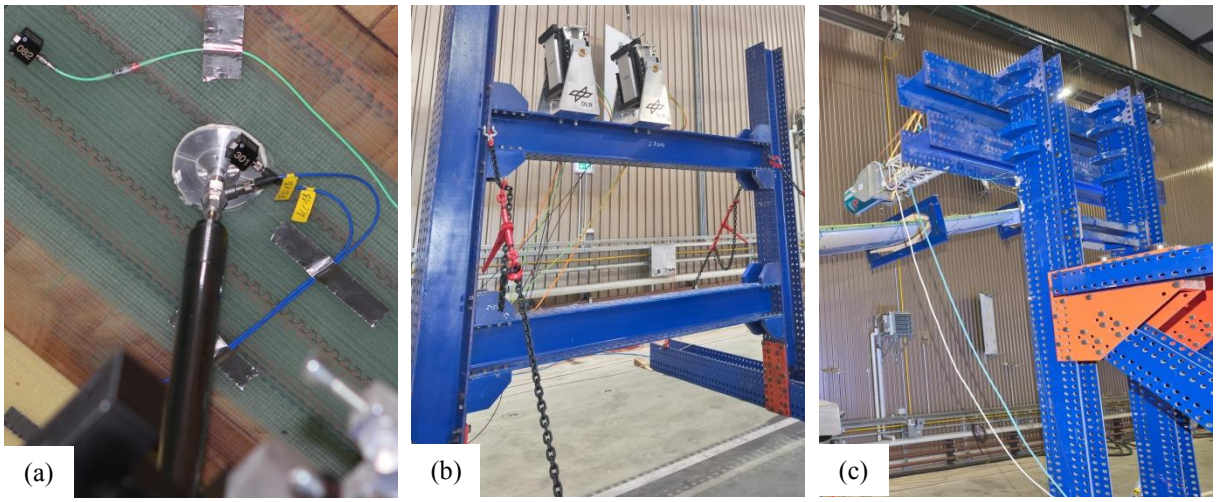

Figure 2. Blade excitation by use of electrodynamic shakers: attachment to the blade surface with mixed adhesive (a), support platforms for flapwise (b) and edgewise (c) loading.

In-phase multi-point excitation has been carried out for flapwise excitation solely. In that case a second shaker of equal type is attached to the blade shell at the same length coordinate but shifted 0.9 m towards the trailing edge. Using Single Virtual Driving Point (SVDP) processing, data from correlated multi-point swept sine excitation is stored directly into single columns of frequency response functions (FRFs) [14]. These FRFs do not deviate from those generated in single-point excitation runs but they are related to a virtual force that acts on a virtual, physically non-existent driving point. The method of SVDP processing is stated on the concept of equivalent complex powers, either generated from two correlated shakers or the virtual force acting on the virtual driving point.

Several test runs with different amplitude levels have been carried out for each excitation setup. The maximum forces that are induced at a single point are 800 N and 340 N for flapwise and edgewise excitation, respectively. As pictured in Figure 2(a), the attachment between rod and blade surface is built from multi-part adhesive, spread over a circular aluminium adapter with a diameter of 6 cm. Given that shear forces are low, the attachment solution is capable of transferring the above mentioned normal forces easily. Detaching between rod and surface as observed in cognate studies (cf. [5]) has not occurred.

The sensor installation is adapted from the free-free test but the resolution is increased to 288 acceleration signals. The number of instrumented sections is raised to 29 and the number of measurement points along the chord length is set to six positions. In 15 sections sensors are placed on the suction side as well. Additional sensors are spent on the test rig to identify possible motion that may have an impact on the structural dynamic behaviour of the blade. For this sake, the test rig is also excited in lateral direction using an impulse hammer. Unfortunately, the overall mass of the instrumentation affects the dynamic properties of the blade considerably. The entire cabling is routed to the blade root from where it is distributed to the measurement system. By weighing the installation components, the total mass assigned to the modal test has been approximated to 46 kg. This includes accelerometers (7.6 kg), connection cables between sensors and patch panels (7.8 kg), patch panels (9.2 kg), and connection cables from the panels to the blade root (21.4 kg). Apart from the modal test

equipment, the blade is loaded with strain gauges and their cabling from the static extreme load tests carried out by IWES. The response signals from the strain gauges have been measured during the modal test but their output is not addressed in this paper. Related additional masses are assumed to be 62 kg. Summarised the installation mass is rated to 108 kg with a recomposed centre of gravity at 6.96 m.

2.3. Aspects of modal analysis

The identification of modal parameters is accomplished by using the PolyMAX frequency domain method (cf. [15]) which is implemented in the LMS Test.Lab environment. In case of shaker excitation, time data signal processing is done with DLR in-house tools that interact with LMS software. From the amount of all measurement runs, each mode shape can be identified several times. They are stored together with the other modal parameters and related metadata into an SQL database. Accessing the database, modes with identical properties coming from different runs are grouped in so-called mode families. For each family, a single mode is selected as the master mode according to various quality measures. Besides the Mode Indicator Function (MIF), considered quality criteria are scalars evaluating phase purity like Modal Phase Collinearity (MPC) and Mean Phase Deviation (MPD), the level of excitation in terms of participation factors, and the generalised force of excitation (cf. [16]). The final modal model represents the collection of all selected master modes.

3. Assorted Results

In Figure 3 some eigenforms which have been determined in experiments at the test rig are displayed. Since the bend-twist coupling is realised geometrically, measured coupling in the lowermost mode shapes is minor compared to structurally modified blades. Nevertheless, there is not negligible flapwise deformation in the 1st edgewise bending shape (Fig. 3(b)) and a significant torsional contribution in the 2nd bending edgewise (Fig. 3(e)) eigenform. An eigenform involving lateral motion of the test rig occurs at a rather low frequency. Its impact on other modal parameters has to be assessed model-based.

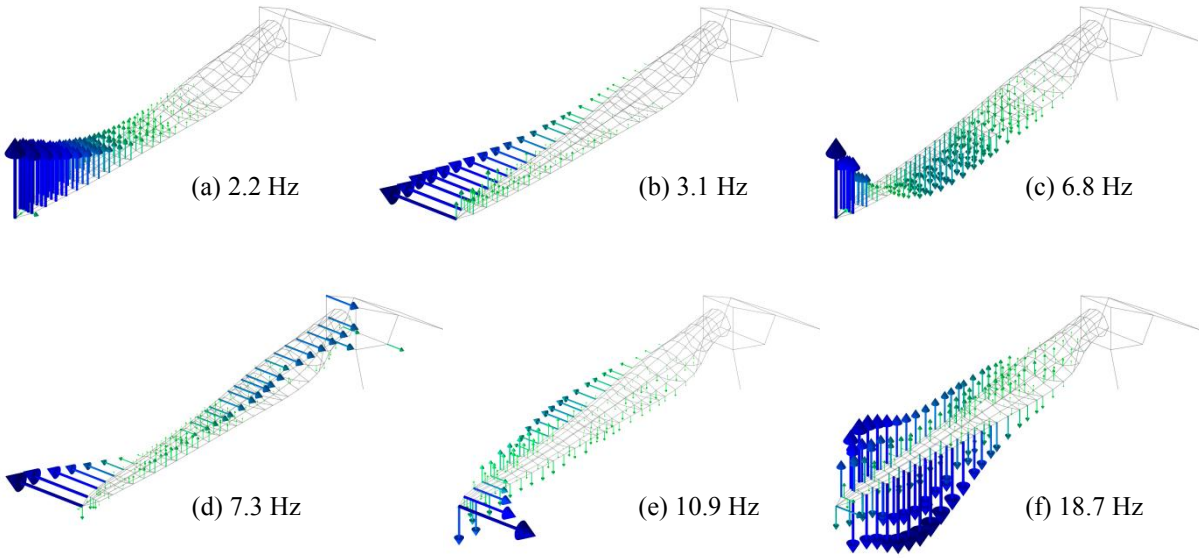

Figure 3. Choice of mode shapes identified at test rig: 1st bending flapwise (a) and edgewise (b), 2nd bending flapwise (c), test rig lateral (d), 2nd bending edgewise (e), and 1st torsion (f). Illustration based on [10].

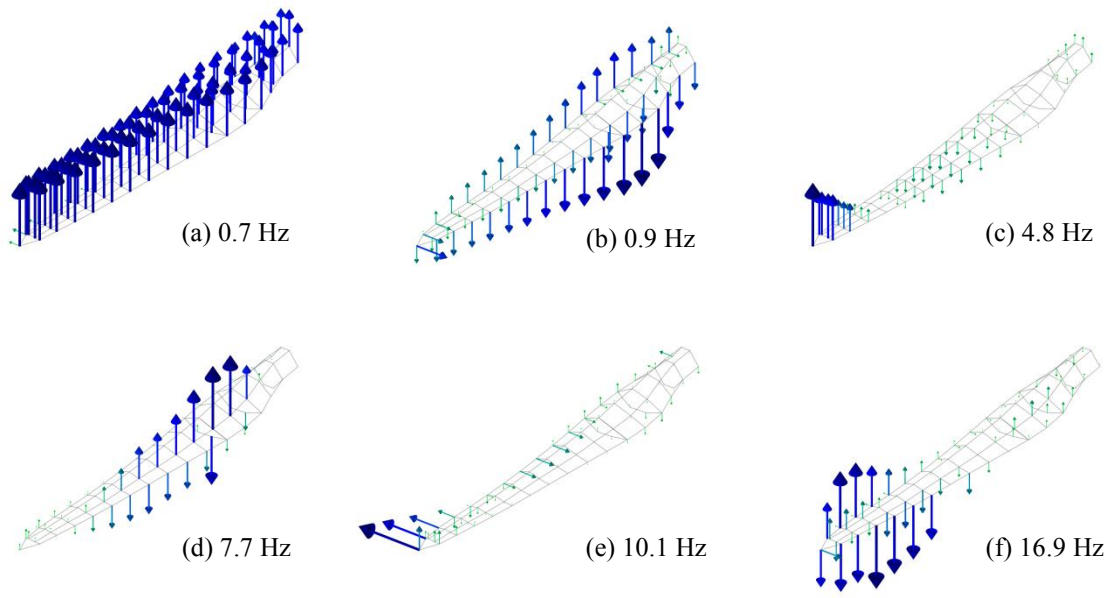

Figure 4. Choice of mode shapes identified in free-free tests of blade #1: rigid body modes of heave (a) and roll (b), 1st bending flapwise (c), breathing of blade (d), 1st bending edgewise (e), and 1st torsion (f). Illustration based on [10].

A compilation of rigid body and elastic mode shapes determined in the free-free test of blade #1 is presented in Figure 4. Apart from mode shapes describing the typical global deformation of rotor blades, local eigenforms of the shells have been identified. They are denoted as the breathing of the blade (Fig. 4(d)). Variable breathing eigenforms have been observed in the modal models emerging from every modal test, also at the test rig, but they are not further examined in the scope of this report. Except for the breathing modes, the test results correlate well with predictions coming from FE modal analysis (cf. [10]).

3.1. Comparison of free-free modal tests

The experiments in free boundary conditions are evaluated in terms of the 10 eigenforms displayed in Table 3. The listing provides an overview of averaged frequencies and modal damping for finished and unfinished blades. Three rigid body modes are illustrated with the only purpose to point out the similarity of the boundary condition within all modal tests. Comparing the modal properties of the rigid body modes is meaningless, because the number of individual rubber bands has been altered.

Table 3. Arithmetic averages of eigenfrequencies and damping values of the blades with and without finish.

mode no.	mode description	eigenfrequency in Hz		diff. in %	modal damping in %		diff. in %
		w/o finish	w/ finish		w/o finish	w/ finish	
1	rigid body heave	0.75	0.70	-6.7	2.86	2.53	-11.5
2	rigid body roll	0.86	0.84	-1.7	2.27	2.51	10.6
3	rigid body pitch	1.04	0.98	-5.8	3.90	3.19	-18.2
4	1st bend. flapwise	4.78	4.72	-1.3	0.24	0.26	8.3
5	1st bend. edgewise	10.29	9.81	-4.7	0.31	0.38	22.6
6	2nd bend. flapwise	11.99	11.87	-1.0	0.38	0.23	-39.5
7	1st torsion	17.24	17.14	-0.6	0.88	0.56	-36.4
8	3rd bend. flapwise	21.00	20.58	-2.0	0.45	0.36	-20.0
9	2nd bend. edgewise	27.86	26.67	-4.3	0.55	0.45	-18.2
10	2nd torsion	28.14	28.69	2.0	0.74	0.47	-36.5

Regarding the elastic modes (no. ≥4), the mass increase caused by the finishing process reduces the majority of eigenfrequencies. Apparently edgewise bending modes are more affected than others. Except for the first bending modes, damping decreases due to the finishing. It should be noted that the overlap of the samples with and without finish concerns only two exemplars. The comparison of the two states assumes nominally equivalent copies of the blades.
Since this assumption is not necessarily met, the frequency and damping values are broken down on each blade separately in Figure 5 and Figure 6. Focusing on the elastic modes of the unfinished blades, one detects that blade #1 stands out from the remaining blades: in both edgewise bending modes and the first torsion mode blade #1 underestimates the average frequency significantly and in the majority of modes it overestimates the damping values. Insofar the decrease in damping associated to the finishing process as displayed in Table 3 should be registered with caution.

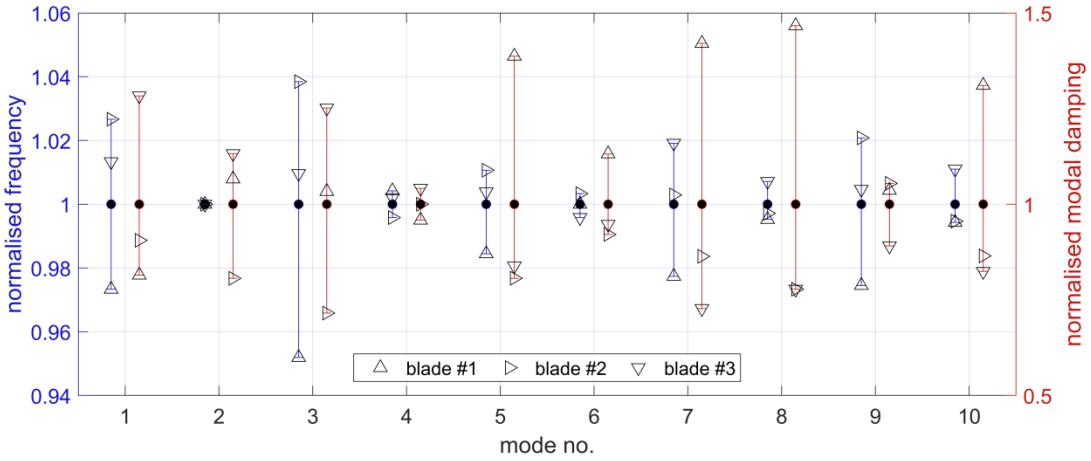

Figure 5. Normalised frequency and damping values of the blades being unfinished.

Generally the similarity amongst the finished blades is higher compared to the unfinished ones. The finishing changes however the individual results of blade #2 and blade #3. For instance, in the unfinished state the eigenfrequency of the 1st torsion mode (no. 7) of blade #3 is slightly higher than of blade #2 whereas after finishing it is the opposite way. The damping values of the 1st edgewise mode (no. 5) are almost equal when the blades are still unfinished, but a huge difference occurs after finishing. Other modes like the 2nd bending edgewise (no. 9) or the 2nd torsion mode (no. 10) indicate notable changes as well. Mode shapes in flap direction exhibit for this blade design less variance in frequency and modal damping attributed to the finishing process.

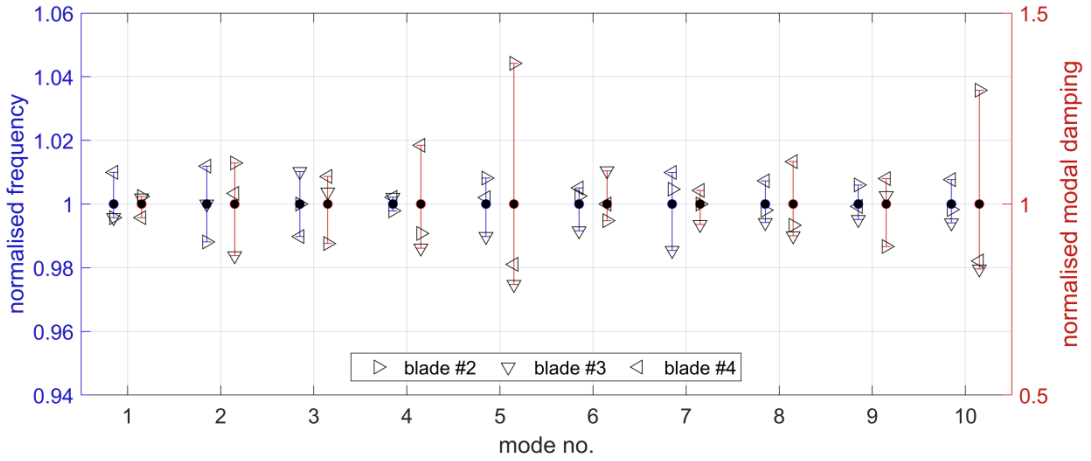

Figure 6. Normalised frequency and damping values of the finished blades.

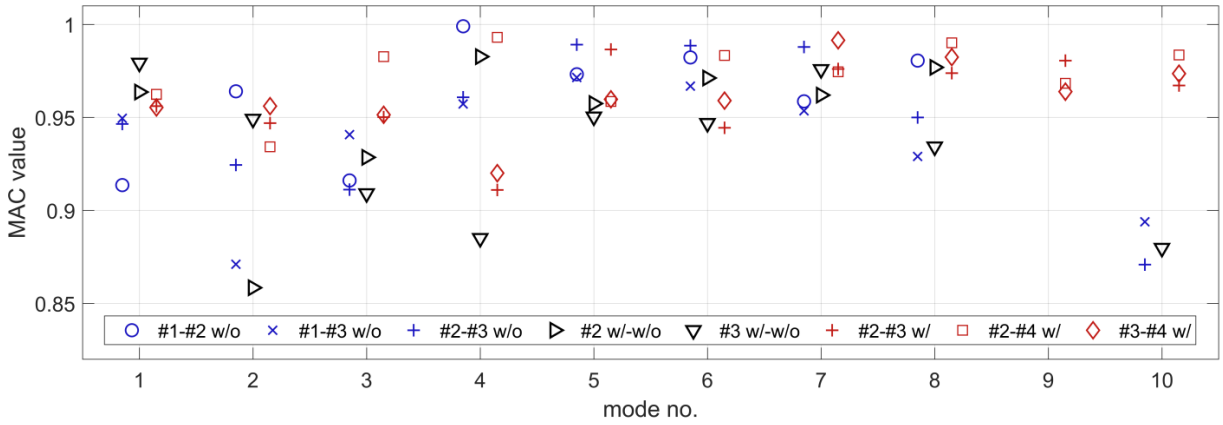

Figure 7. Overview of MAC values for different correlated combinations.

Of vital importance is a sound agreement of mode shape vectors as such. This is commonly evaluated by means of the modal assurance criterion (MAC). The diagram in Figure 7 shows MAC values comparing eigenforms of eight reasonable combinations, i.e. the blades with and without finish amongst each other, and blade #2 and blade #3 in the two different states. From the overview follows that the blades without finish correlate somewhat better in the first three elastic modes, but for higher modes the finished blades yield a clearly improved correlation. In particular for the 2nd edgewise mode any different combination outside of the finished set coincides poorly (<0.8). Interesting results are obtained for the correlation of the two blades before and after finishing. Alterations in the mode shape due to the finish appear also for lower modes. In case of blade #3 the 1st flapwise bending mode is degenerated in correlation by more than 10%. Nonetheless, for higher frequencies and thus mode shape numbers the differences induced by the finish become particularly noticeable.

3.2. On possible non-linearity of the rotor blade

In test rig fixation different force levels have been applied to investigate the blade in larger deformations. Of interest are possible changes of modal parameters due to non-linear behaviour. Figure 8 presents results of this approach for the 1st flap mode. The plots display the maximum tip displacement during sinusoidal sweeps, eigenfrequency of the mode, and modal damping as a function of the generalised induced force in modal domain. The discrete values are obtained from eight independent test runs belonging to the same mode family. If the structure responded entirely linear the relationship to tip displacement would be a straight line. Here, the gradient between tip displacement and generalised force declines slowly, which represents a deviation from linearity.

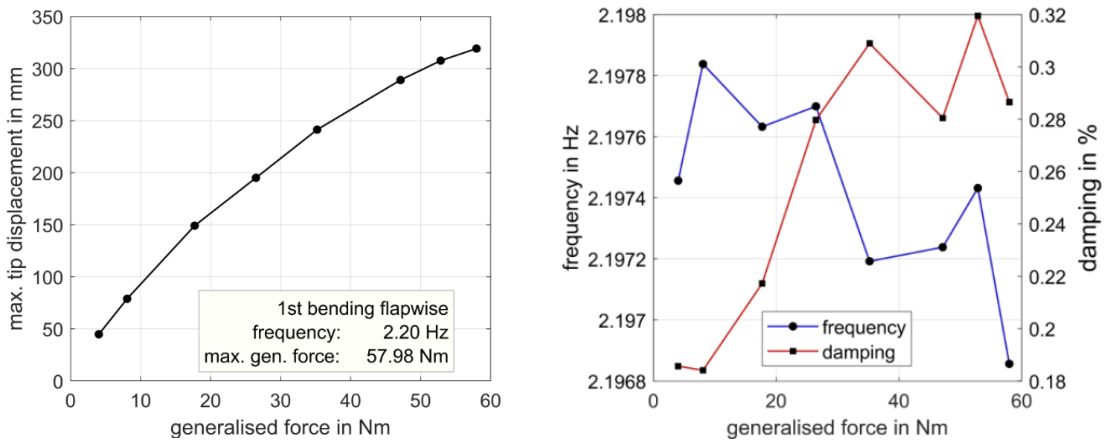

Figure 8. Linearity plots for 1st bending flapwise.

Deviations from linearity may for example evolve from variable modal stiffness or damping. As illustrated in the right plot of Fig. 8, the frequency and therewith stiffness is rather constant whereas a major increase in damping can be observed. Such information is crucial in order to assess the aeroelastic phenomenon of flutter, where higher deflections of the blade occur.

4. Summary and Conclusions

In this report peculiarities concerning the realisation of modal tests of rotor blades in two boundary conditions are presented. The outlined test setups are the most conceivable options in a quasi-industrial setting.

In every test final modal models have been determined out of several excitation runs according to meaningful quality measures. Obtained results from multiple free-free tests allow for conclusions concerning effects of the finishing and the repeatability of the manufacturing process in terms of the modal parameters. For this blade series the impact of the finish on mode shape correlation is stronger than differences resulting from the production. Regarding frequency and damping, changes caused by the finishing and deviations between the blades within the same manufacturing steps are of a similar magnitude. For blade #1 a non-linear damping behaviour in the 1st flap mode has been identified. Though, a comprehensive flutter analysis demands in preparation the examination on non-linear behaviour in other modes of interest. Due to the high sensor density and the advantages of both test scenarios, the acquired modal data represents an optimal basis for updating finite element models towards structural dynamic properties.

Although applied on a 20 m demo blade, the utilisation of all illustrated techniques on a full-scale structure is feasible. The described advantages and drawbacks of the portrayed test scenarios persist for larger sizes and higher weights of rotor blades. Depending on the blade properties, it is however inevitable to customise certain aspects for each test individually. This includes for instance the adjustment of the suspension system in free-free tests or the optimal choice of excitation points in tests using electrodynamic shakers. Suchlike issues should be accounted for in a pretest analysis incorporating the respective finite element model.

Acknowledgements

This work was partially funded by the German Federal Ministry for Economic Affairs and Energy (BMWi) in the SmartBlades2 project (0324032A-H). The authors are much obliged to all members of the modal test team, and to the on-site support provided by Fraunhofer IWES, Bremerhaven and NWTC, Boulder.

References

[1] Wind turbines - Part 23: Full-scale structural testing of rotor blades 2014 *IEC 61400-23*

[2] Larsen G C *et al* 2002 Modal analysis of wind turbine blades *Risoe-R* 1181(EN)

[3] Griffith D T *et al* 2008 Modal testing for validation of blade models *Wind Engineering* **32(2)** pp 91-102

[4] Luczak M *et al* 2014 Updating finite element model of a wind turbine blade section using experimental modal analysis results *Shock and Vibration* AID 684786

[5] Luczak M *et al* 2018 Research sized wind turbine blade modal tests: comparison of the impact excitation with shaker excitation *J. Phys.: Conf. Series* **1102** 012022

[6] Griffith D T and Carne TG 2006 Experimental uncertainty quantification of a class of wind turbine blades *Proc. of the IMAC-XXIV*

[7] Homepage of SmartBlades2 project [online] Available: www.smartblades.info [latest access on 12 26 2018]

[8] Govers Y *et al* 2014 Airbus A350XWB ground vibration testing: efficient techniques for customer oriented on-site modal identification *Proc. of ISMA*

[9] Göge D *et al* 2007 Ground vibration testing of large aircraft - state-of-the-art and future prespectives *Proc. of the IMAC-XXV*

[10] Gundlach J and Govers Y 2018 Experimentelle Modalanalyse an einem aeroelastisch optimierten Rotorblatt mit Biege-Torsions-Kopplung im Projekt SmartBlades2 *VDI-Berichte* **2323** pp 91-104

[11] Rotor blades for wind turbines 2015 *DNVGL-ST-0376*

[12] Mottershead J E and Friswell M 1995 *Finite element model updating in structural dynamics*, Kluwer Academic Publishers

[13] Giclais S *et al* 2011 New excitation signals for aircraft ground vibration testing *15th Int. forum on aeroelasticity and structural dynamics* IFASD 136

[14] Füllekrug U *et al* 2008 Measurement of FRFs and modal identification in case of correlated multi-point excitation *Shock and Vibration* **15** pp 435-445

[15] Peeters B 2004 The PolyMAX frequency-domain method_a new standard for modal parameter estimation? *Shock and Vibration* **11** pp 395-409

[16] Heylen W *et al* 1998 *Modal Analysis Theory and Testing* KU Leuven